Pancreatology 23 (2023) 911–918

Contents lists available at ScienceDirect

Pancreatology

journal homepage: www.elsevier.com/locate/pan

Decreased neutrophil counts prolong inflammation in acute pancreatitis and cause inflammation spillover to distant organs

Yohei Fukuda [a, 1], Kosuke Mori [b, 1], Hideshi Okada [a, c, *, 2], Hiroyuki Tomita [b, c, **, 2], Kodai Suzuki [a], Chihiro Takada [a], Ryo Kamidani [a], Yuki Kawasaki [a], Hirotsugu Fukuda [a], Toru Minamiyama [a], Ayane Nishio [a], Takuto Shimada [a], Ayumi Kuroda [a], Akihiro Uchida [a], Yuichiro Kitagawa [a], Tetsuya Fukuta [a], Takahito Miyake [a], Takahiro Yoshida [a], Akio Suzuki [d], Nobuyuki Tetsuka [e], Shozo Yoshida [a, f], Shinji Ogura [a]

[a] Department of Emergency and Disaster Medicine, Gifu University Graduate School of Medicine, Japan
[b] Department of Tumor Pathology, Gifu University Graduate School of Medicine, Japan
[c] Center for One Medicine Innovative Translational Research, Gifu University Institute for Advanced Study, Japan
[d] Department of Pharmacy, Gifu University Hospital, Japan
[e] Department of Infection Control, Gifu University Graduate School of Medicine, Japan
[f] Abuse Prevention Emergency Medicine, Gifu University Graduate School of Medicine, Gifu, Japan

ARTICLE INFO

Article history:
Received 31 March 2023
Received in revised form
18 July 2023
Accepted 26 October 2023
Available online 3 November 2023

Keywords:
Animal study
Inflammatory response
Neutrophils
Pancreas

ABSTRACT

Background/objective: Acute pancreatitis is an aseptic inflammation caused by pathologically activated pancreatic enzymes and inflammatory mediators produced secondarily by neutrophils and other inflammatory cells and is one of the most difficult diseases to treat. This study aimed to investigate the role of neutrophils in pancreatitis by examining tissue dynamics.
Methods: We created a model of caerulein-induced pancreatitis in 12-week-old male granulocyte colony-stimulating factor knockout mice (G−CSF−KO) and wild-type littermate control mice (six intraperitoneal injections of caerulein [80 μg/kg body weight] at hourly intervals for 2 days). Mice were sacrificed 0, 3, 6, 12, 24, 36, 48, 72, and 168 h after caerulein administration and examined histologically.
Results: The survival rate after one week of caerulein administration was 100 % in the control mice, whereas it was significantly lower (10 %) in the G−CSF−KO mice. Histological examination revealed significant hemorrhage and inflammatory cell migration in the G−CSF−KO mice, indicating prolonged inflammation.
Conclusion: Prolonged inflammation was observed in the G−CSF−KO mice. Tissue cleanup by neutrophils during the acute phase of inflammation may influence healing through the chronic phase.

1. Introduction

Neutrophils are the major phagocytic granulocytes responsible for innate immunity. They are the most abundant type of granulocytes, constituting up to 60 % of all white blood cells in humans [1], and form an essential part of the innate immune system. Neutrophils phagocytose pathogens in response to pathogen- and damage-associated molecular patterns [2]. In addition, neutrophils facilitate immune responses by releasing granules, producing cytokines, and mediating the mobilization of other immune cells to the site of infection.

Nevertheless, when the immune response is excessive, neutrophils can cause considerable damage to the host, including extensive cell death, necrosis, vascular leakage, thrombus formation, and antibody-mediated autoimmune reactions. In fact, neutrophils are considered to play a pivotal role in the aggravation of acute respiratory distress syndrome (ARDS); neutrophil activation and

* Corresponding author. Department of Emergency and Disaster Medicine, Gifu University Graduate School of Medicine, 1-1 Yanagido, Gifu, 501-1194, Japan.
** Corresponding author. Department of Tumor Pathology, Gifu University Graduate School of Medicine, 1-1 Yanagido, Gifu, 501-1194, Japan.
E-mail addresses: okada.hideshi.a4@f.gifu-u.ac.jp (H. Okada), tomita.hiroyuki.y6@f.gifu-u.ac.jp (H. Tomita).
[1] Yohei Fukuda and Kosuke Mori contributed equally to this manuscript.
[2] Hideshi Okada and Hiroyuki Tomita contributed equally to the Correspondence.

https://doi.org/10.1016/j.pan.2023.10.020

transmigration are hallmark events in the progression of this disease [3]. In addition, neutrophil elastase (NE), which is produced by neutrophils, has been previously reported to play a pivotal role in the pathogenesis of acute lung injury/ARDS [4], and elevated NE levels are correlated with the severity of lung injury [5–7]. Conversely, neutropenia has been shown to produce a protective effect against endotoxemia in mice, and the amount of neutrophil-secreted mediators was insufficient to cause endothelial injury in a previous report [8,9]. On the other hand, since neutrophils are one of the first inflammatory cells to migrate toward the site of inflammation during the acute phase of inflammation, particularly as a result of bacterial infection, environmental exposure and moderate inflammation are also known to be necessary for tissue repair [10].

Acute pancreatitis is an aseptic inflammation caused by pathologically activated pancreatic enzymes and is characterized by pathological changes such as edema, hemorrhage, and necrosis in the pancreas [11]. The cascade reaction caused by the pancreatic enzymes activated in the pancreas and inflammatory mediators produced secondarily by inflammatory cells such as neutrophils is amplified in severe pancreatitis, causing them to overflow into the extrapancreatic space and expanding the inflammatory reaction outside the pancreas [12]. In mild-to-moderate cases, the fatality rate is a few percent; however, in cases involving severe acute pancreatitis, the fatality rate is reported to be 20 % [13–15]. Likewise, acute pancreatitis often develops into chronic pancreatitis [16,17].

In this study, we used granulocyte colony-stimulating factor knockout mice to determine the functions of neutrophils in a moderate pancreatitis mouse model in which inflammation ended in three weeks.

2. Methods

2.1. In vivo animal studies

This study conformed to the Guide for the Care and Use of Laboratory Animals published by the US National Institutes of Health (NIH publication, 8th Edition, 2011) and was approved by the Institutional Animal Research Committee of Gifu University (2022-053, Gifu, Japan). Male granulocyte colony-stimulating factor (G–CSF)–deficient mice (B6; 129P2-Csf3tm1Ard/J) were purchased from Jackson Laboratory (Bar Harbor, ME, USA) and bred as described previously [18]. G-CSF genotypes have been described previously [18,19]. G-CSF induces the appearance of colonies containing only granulocytes. Thus, G–CSF–knockout (G–CSF–KO) mice show chronic neutropenia, granulocyte and macrophage progenitor cell deficiencies, and impaired neutrophil mobilization [18]. Although approximately 50 % of G–CSF–KO mice die in utero, the surviving mice grow to adulthood [18]. Wild-type littermate mice were used as controls.

Acute pancreatitis was induced in vivo by administering the secretagogue caerulein (Sigma, Louis, MO, USA) in six intraperitoneal injections of 80 μg/kg body weight at hourly intervals for 2 days. The survival rate was determined one week after caerulein administration.

Perfusion fixation and blood sampling from the ophthalmic artery were performed under anesthesia (intraperitoneal mixture of medetomidine hydrochloride 0.3 mg/kg, midazolam [4 mg/kg], and butorphanol tartrate [5 mg/kg]). Anesthesia was deemed sufficient if corneal and hind-paw withdrawal reflexes were absent. Mice were euthanized by exsanguination from the ophthalmic artery until the lighting reflex was lost and heart specimens were obtained subsequently.

2.2. Flow cytometry analysis of peripheral neutrophils

To profile G–CSF–KO mice, peripheral neutrophil numbers were analyzed, and blood samples were collected from the maxillary artery. The samples were prepared as described previously [9]. Cells were stained with the following antibodies (BioLegend, San Diego, CA, USA) for 5 min at room temperature: anti-mouse CD45–peridinin chlorophyll protein complex (clone: 30-F11), anti-mouse CD11b-phycoerythrin (clone: M1/70), anti-mouse Ly6G-fluorescein isothiocyanate (clone: 1A8), and anti-mouse F4/80-Alexa Fluor 647 (clone: BM8). Neutrophils were defined as CD45 + CD11b + Ly6G + F4/80− white blood cells. Flow cytometry was performed on a BD FACSCalibur instrument (Becton and Dickinson Company, Franklin Lakes, NJ, USA), and data were analyzed using FlowJo software, version 10.5.3 (TreeStar LLC, Ashland, OR, USA).

2.3. Flow cytometry analysis of the pancreatic tissue

Pancreatic cells of wild-type (n = 3) and G–CSF–KO (n = 3) mice at eight weeks of age were isolated from the pancreas tissue. Briefly, the pancreatic tissue was minced into small fragments and harvested using the Horizon Dri Tumor and Tissue Dissociation Reagent (TTDR, Cat#661563, BD Biosciences, Franklin Lakes, NJ, USA), according to the manufacturer's protocol. All isolated pancreatic cells were subjected to flow-cytometry analysis. Briefly, to prevent non-specific Fc binding, single-cell suspensions of all pancreatic cells were incubated with Fc Block (Cat#553143, BD Biosciences). Then, cells were incubated with the appropriate antibodies: CD45.2 FITC (Cat# 109805, BioLegend), Ly6G APC/Cyanine7 (Cat# 127623, BioLegend), CD11b APC (Cat# 101221, BioLegend), CD11b APC/Cyanine7 (Cat# 101225, BioLegend), F4/80 APC (Cat# 123115, BioLegend), CD11c APC/Cyanine7 (Cat# 117323, BioLegend), MHCII (I-A/I-E) APC (Cat# 107613, BioLegend), CD4 PerCP/Cy5.5 (Cat# 100433, BioLegend), and CD8a PerCP/Cy5.5 (Cat# 100733, BioLegend). Dead cells were stained with the SYTOX Red Dead Cell Stain (Cat# MP34859, Invitrogen, Waltham, MA, USA) or Propidium Iodide Staining Solution (Cat# 556463, BD Pharmagen, San Diego, CA, USA). The samples were analyzed on the CytoFLEX S Flow Cytometry System (Beckman Coulter, Brea, CA, USA) and analyzed using FlowJo software, version 10.8 (Tree Star Inc., Ashland, OR, USA).

2.4. Histopathological examination

The pancreas and whole right lobe of the lungs from six individual mice at 0, 3, 24, 36, 72, and 168 h after caerulein administration were fixed with PBS containing 10 % formalin and embedded in paraffin. Paraffin sections (4 μm) were deparaffinized and rehydrated. Finally, slides were counterstained with hematoxylin and eosin, and the coverslipped pancreas sections were scored for pancreatic edema as follows: 0 = absent; 0.5 = focal expansion of interlobar septae; 1 = diffuse expansion of interlobar septae; 1.5 = same as 1 + focal expansion of interlobular septae; 2 = diffuse expansion of interlobar septae; 2.5 = same as 2 + focal expansion of interacinar septae; 3 = same as 2 + diffuse expansion of interacinar septae; 3.5 = same as 3 + focal expansion of intercellular spaces; or 4 = same as 3 + diffuse expansion of intercellular spaces. Acinar necrosis was scored as follows: 0 = absent; 0.5 = focal occurrence of 1–4 necrotic cells/high-power field (HPF); 1 = diffuse occurrence of 1–4 necrotic cells/HPF; 1.5 = same as 1 + focal occurrence of 5–10 necrotic cells/HPF; 2 = diffuse occurrence of 5–10 necrotic cells/HPF; 2.5 = same as 2 + focal occurrence of 11–16 necrotic cells/HPF; 3 = diffuse occurrence of 11–16 necrotic cells/HPF (foci of confluent necrosis); 3.5 = same as

3 + focal occurrence of >16 necrotic cells/HPF; or 4 = >16 necrotic cells/HPF (extensive confluent necrosis). Hemorrhage and fat necrosis were scored as follows: 0 = absent; 0.5 = 1 focus, 1 = 2 foci; 1.5 = 3 foci, 2 = 4 foci; 2.5 = 5 foci, 3 = 6 foci; 3.5 = 7 foci, or 4 = 8 or more foci. Inflammation and perivascular infiltrate were scored as follows: 0 = 0–1 intralobular or perivascular leukocytes/HPF; 0.5 = 2–5 intralobular or perivascular leukocytes/HPF; 1 = 6–10 intralobular or perivascular leukocytes/HPF; 1.5 = 11–15 intralobular or perivascular leukocytes/HPF; 2 = 16–20 intralobular or perivascular leukocytes/HPF; 2.5 = 21–25 intralobular or perivascular leukocytes/HPF; 3 = 26–30 intralobular or perivascular leukocytes/HPF; 3.5 = more than 30 leukocytes/HPF or focal microabscesses; or 4 = more than 35 leukocytes/HPF or confluent microabscesses [11]. Scoring was performed manually as 10 HPF per sample (n = 6 per sample) in the focal plane.

The coverslipped lung sections were scored as follows for pulmonary edema: 1, absent; 2, detectable seroproteinaceous fluid in one to a few alveoli; or 3, seroproteinaceous fluid-filled alveoli in a multifocal-to-coalescing pattern in the lungs. Neutrophilic infiltration was scored as follows: 1, absent or rare solitary neutrophils; 2, detectable extravasated neutrophils observed as small loose cellular aggregates in one or a few airways and/or alveoli; 3, detectable extravasated neutrophils observed as loose-to-compact cellular aggregates in multiple to coalescing airways and/or alveoli with some effacement of lung architecture; or 4, detectable extravasated neutrophils observed as compact cellular aggregates effacing most of the adjacent lung architecture [20]. These assessments were performed in a blinded manner to avoid bias.

2.5. Measurement of serum amylase levels

Serum amylase concentrations were measured by ORIENTAL YEAST Co., Ltd. (Tokyo, Japan) at 0, 3, 6, 12, 18, 24, 36, 48, 72, and 168 h after caerulein administration.

2.6. Immunohistochemistry

After deparaffinization, sections (4 μm) were cut and incubated with primary antibodies against the macrophage marker F4/80 (700765; Cell Signaling, Danvers, MA, USA), CD8 (EPR21769; Abcam, Cambridge, UK), which is a lymphocyte marker, or amylase (12540-1-AP; Proteintech, Rosemont, IL, USA). Target proteins were visualized using the VECTASTAIN Elite ABC system (Vector Laboratories, Newark, CA, USA) or the secondary antibodies (Alexa Fluor 488, Invitrogen).

2.7. Scoring of intensity

For the quantitative analysis of amylase in tissue, scoring of the of amylase antibody was performed using a confocal fluorescence microscope (BZ-X810, Keyence, Osaka, Japan) and ImageJ software (Olympus Corp., Tokyo, Japan) as described previously [21]. The pancreas of each mouse was embedded in an OCT compound and frozen with liquid nitrogen. The frozen blocks were stored at −80 °C, and sections of frozen tissues (5–7-μm thick) were prepared with a cryostat. The intensity of amylase with Alexa Fluor 488 staining was scored manually in 10 HPF per sample (n = 6 per sample) in the focal plane.

2.8. Data and statistical analysis

Data are presented as mean ± SEM. Student's two-tailed *t*-test was used to compare the two groups, and survival data were analyzed using the log-rank test; $P < 0.05$ was considered significant. All calculations were performed using GraphPad Prism, version 7.02 (GraphPad Software, La Jolla, CA, USA).

3. Results

3.1. G–CSF–KO mice with pancreatitis showed a lower survival rate

ELISA analysis indicated serum G-CSF deficiency in G–CSF–KO mice (wild-type: 146.7 ± 21.2 pg/mL vs. G–CSF–KO: 9.7 ± 5.4 pg/mL, $P < 0.01$) (Fig. 1A). In addition, peripheral neutrophil counts obtained using flow cytometry were significantly lower in G–CSF–KO mice than in wild-type mice before caerulein injection (wild-type: 452 ± 29 cells/μL vs. G–CSF–KO: 69 ± 15 cells/μL, $P < 0.01$) (Fig. 1B). These results are consistent with those of a previous study [8,9]. The flow cytometry analysis of immune cells of a normal pancreas revealed that there were few pancreatic immune cells and that the population of immune cells was not significantly different between wild-type and G–CSF–KO mice (Supplementary Fig. 1).

The survival rate 7 days after caerulein administration was significantly lower ($p < 0.05$) among G–CSF–KO mice (3 of 30 mice; 10 %) than among wild-type mice (10 of 10 mice; 100 %) (Fig. 1C).

In wild-type mice, serum amylase levels peaked at 3 h after caerulein administration and then rapidly decreased, returning to pre-caerulein levels by 12 h. The peak serum amylase levels did not differ significantly between G–CSF–KO and wild-type mice (Fig. 1D). In addition, tissue amylase levels were not significantly difference between the G–CSF–KO and wild-type mice (Supplementary Fig. 2).

3.2. Histopathology in pancreatitis

Next, histological evaluation of pancreatitis was performed over time. (Fig. 2A). In wild-type mice, the pancreatic edema score increased 3 h after finishing caerulein administration, and then gradually decreased until one week after caerulein injection (Fig. 2B). Conversely, in G–CSF–KO mice, pancreatic edema was prolonged by 72 h and one week after caerulein administration. Although inflammation and perivascular infiltration increased until 36 h after caerulein administration in wild-type compared with G–CSF–KO mice, inflammation and perivascular infiltration were greater in G–CSF–KO mice 72 h and one week after caerulein injection than in wild-type mice (Fig. 2C).

The acinar necrosis score in wild-type mice increased from 3 h after caerulein administration and gradually decreased from 36 h after caerulein injection. In G–CSF–KO mice, acinar necrosis was larger one week after caerulein administration than in wild-type mice (Fig. 2D). The hemorrhage score gradually increased from 3 h after caerulein injection, whereas it was low in wild-type mice after caerulein administration (Fig. 2E).

3.3. In G–CSF–KO mice, the number of infiltrating inflammatory cells was high despite the absence of granulocytes

Histological analysis was performed to further confirm the profile of the inflammatory cells (Fig. 3A and B). In G–CSF–KO mice, neutrophil counts did not increase over any time range. In addition, neutrophils migrated to areas with some residual glandular tissue, whereas they were rarely found in areas where necrosis had advanced and no glandular tissue remained.

Macrophages that stained positive for F4/80 increased up to 24 h after the end of caerulein administration and then decreased in wild-type mice (Fig. 4A and B). In contrast, fewer F4/80-positive cells were observed in G–CSF–KO mice up to 24 h after caerulein administration, and their numbers increased from 36 h onward in comparison with wild-type mice.

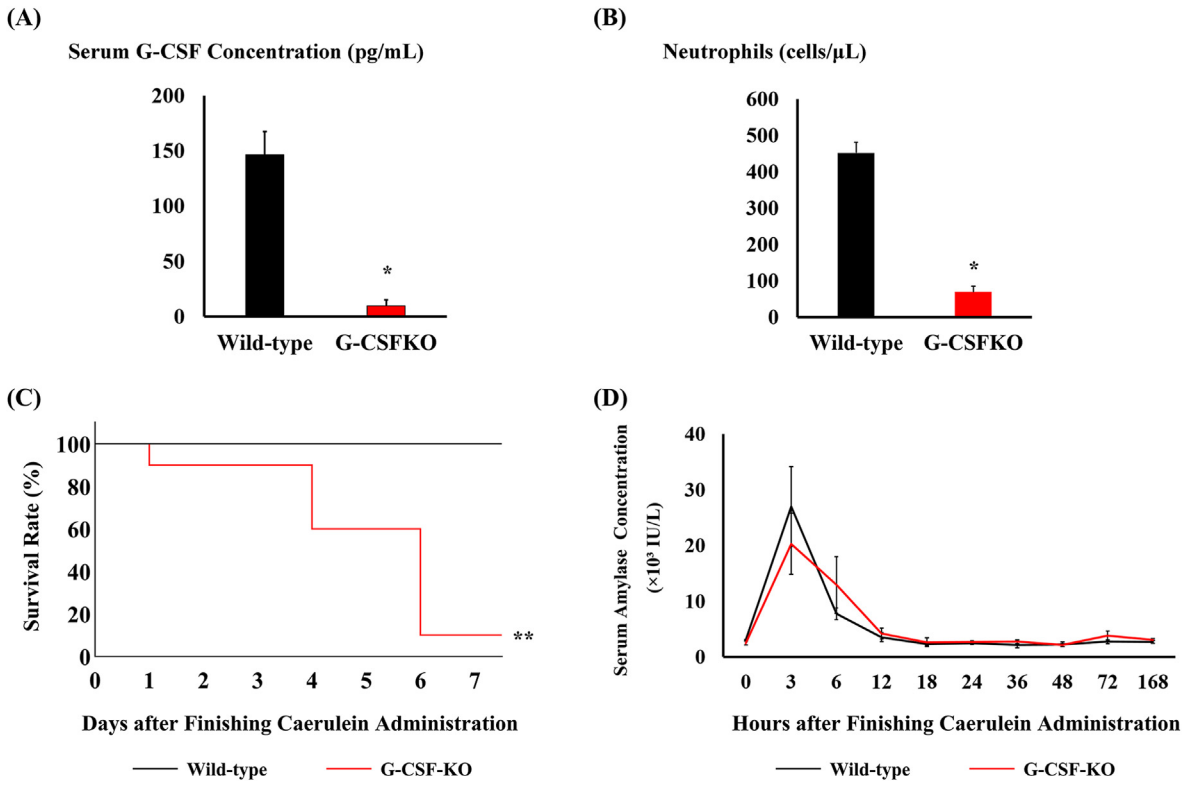

Fig. 1. Granulocyte colony-stimulating factor knockout (G–CSF–KO) mice in caerulein-induced pancreatitis.
A: Serum G-CSF levels in untreated wild-type and G–CSF–KO mice were measured using an enzyme-linked immunosorbent assay. **B:** Peripheral neutrophils ($CD45^+CD11b^+Ly6G^+F4/80^-$) in untreated wild-type and G–CSF–KO mice were quantified by flow cytometry. **C:** Kaplan–Meier survival curves for wild-type and G–CSF–KO mice after caerulein administration. **D:** Serum amylase concentrations were measured over time in both groups of mice. Data are expressed as mean ± SEM. n = 6 mice per group **(A)**; n = 6 mice per group **(B)**; n = 10 wild-type mice **(C)**; and n = 30 G–CSF–KO mice **(C)**. *$P < 0.01$, **$P < 0.05$ versus wild-type.

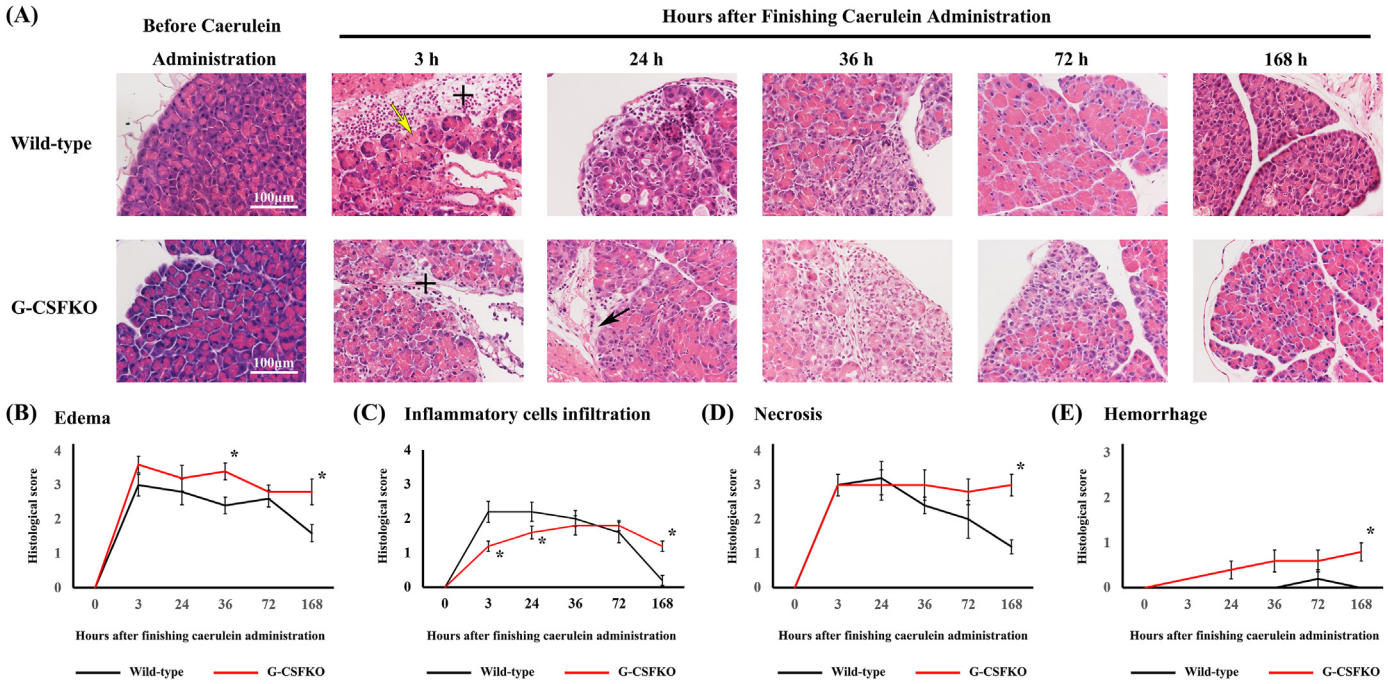

Fig. 2. Histological scores of caerulein-induced pancreatitis.
A: Representative images of hematoxylin and eosin-stained pancreatic tissues over time after caerulein administration. + indicates edema. Yellow arrows indicate the necrosis. The black arrowhead indicates hemorrhage. The graphs present the histological scoring of pancreatic injury related to edema, inflammatory cell infiltration, necrosis, and hemorrhage. **B-E:** Graphs of histological scoring of pancreatic injury, including edema **(B)**, inflammatory cell infiltration **(C)**, necrosis **(D),** and hemorrhage **(E)**. *$P < 0.05$ versus the wild-type.

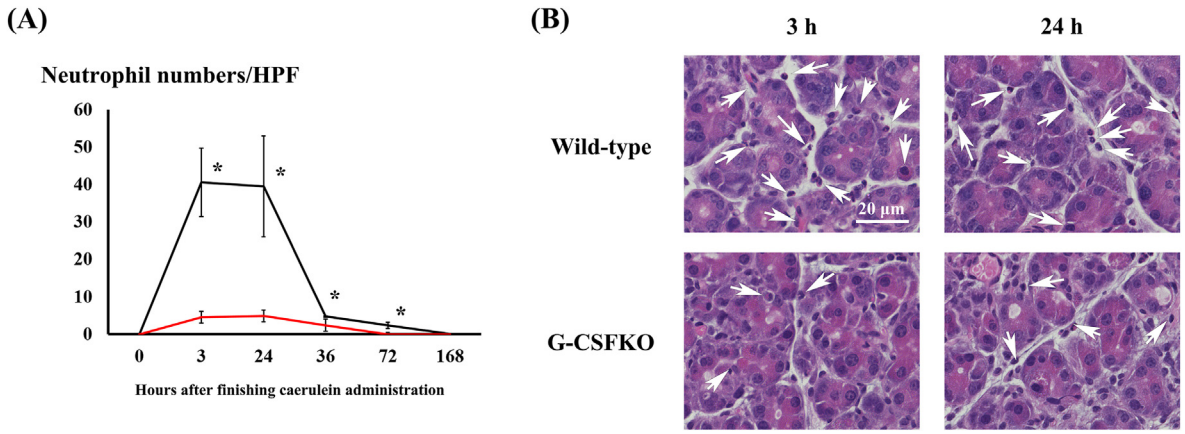

Fig. 3. Neutrophil counts over time in pancreatitis.
A: Graphs of neutrophil numbers over time in the pancreas of wild-type and G–CSF–KO mice. **B:** Representative images of hematoxylin and eosin-stained pancreatic tissues 3 and 24 h after caerulein administration in both groups. Arrows indicate the neutrophils. *$P < 0.01$ versus the wild-type.

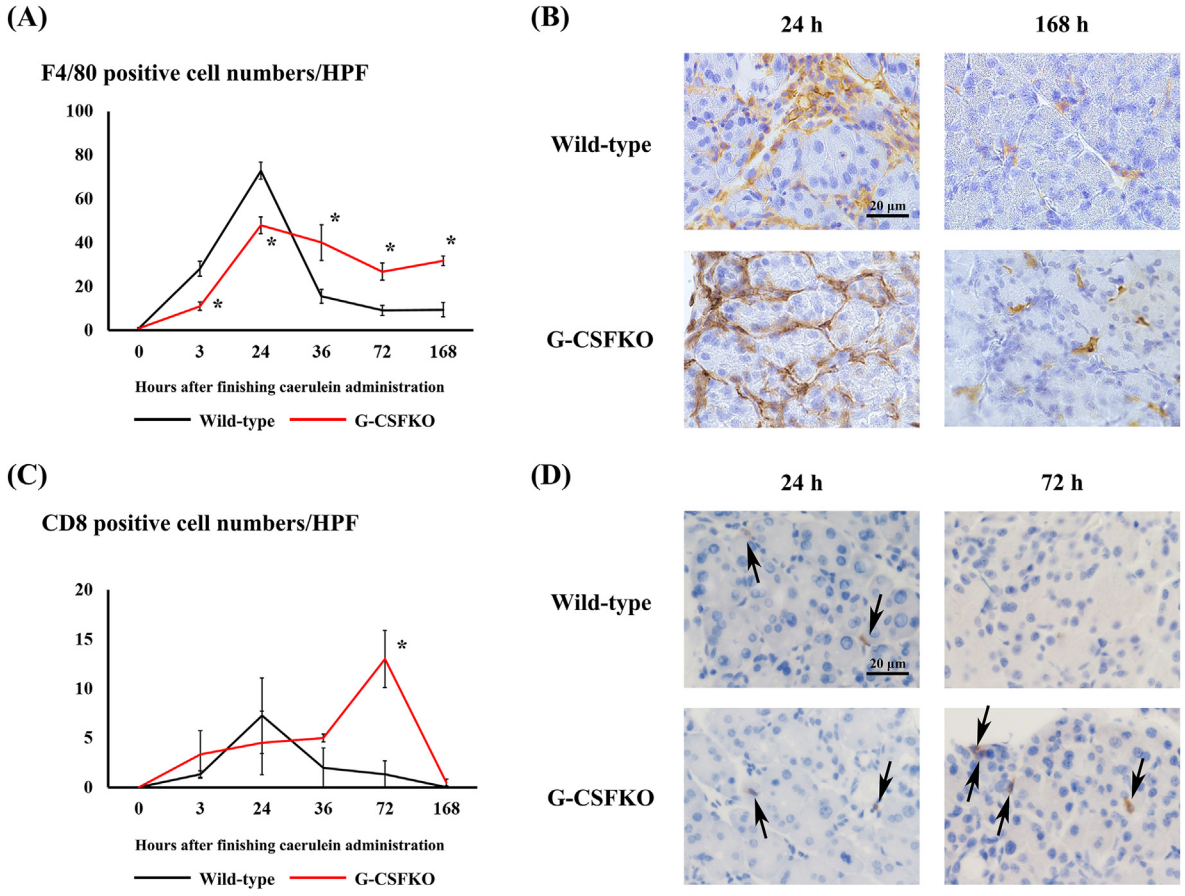

Fig. 4. F4/80- and CD8-positive cell numbers over time in pancreatitis.
A: Graphs of F4/80-positive cell numbers over time in the pancreas of wild-type and G–CSF–KO mice. **B:** Representative images of F4/80-immunostained pancreatic tissues 24 and 168 h after caerulein administration. Arrows indicate F4/80-positive cells. **C:** Graphs of $CD8^+$ cell numbers over time in the pancreas of wild-type and G–CSF–KO mice. **D:** Representative images of CD8-immunostained pancreatic tissues 24 and 168 h after caerulein administration. Arrows indicate CD8-positive cells. *$P < 0.05$, versus the wild-type.

Next, to assess cytotoxic lymphocytes, immunohistochemical analysis was performed over time after administration of caerulein. The number of cytotoxic T cells, which were indicated as $CD8^+$ cells, was investigated (Fig. 4C and D). The number of CD8-positive cells peaked 24 h after the end of caerulein administration in control mice and then declined, whereas it took 72 h for the number of CD8-positive cells to peak in G–CSF–KO mice, which had significantly more CD8-positive cells at this time.

3.4. Examination of effects on remote organs

Next, the effects of prolonged inflammation in the pancreas on

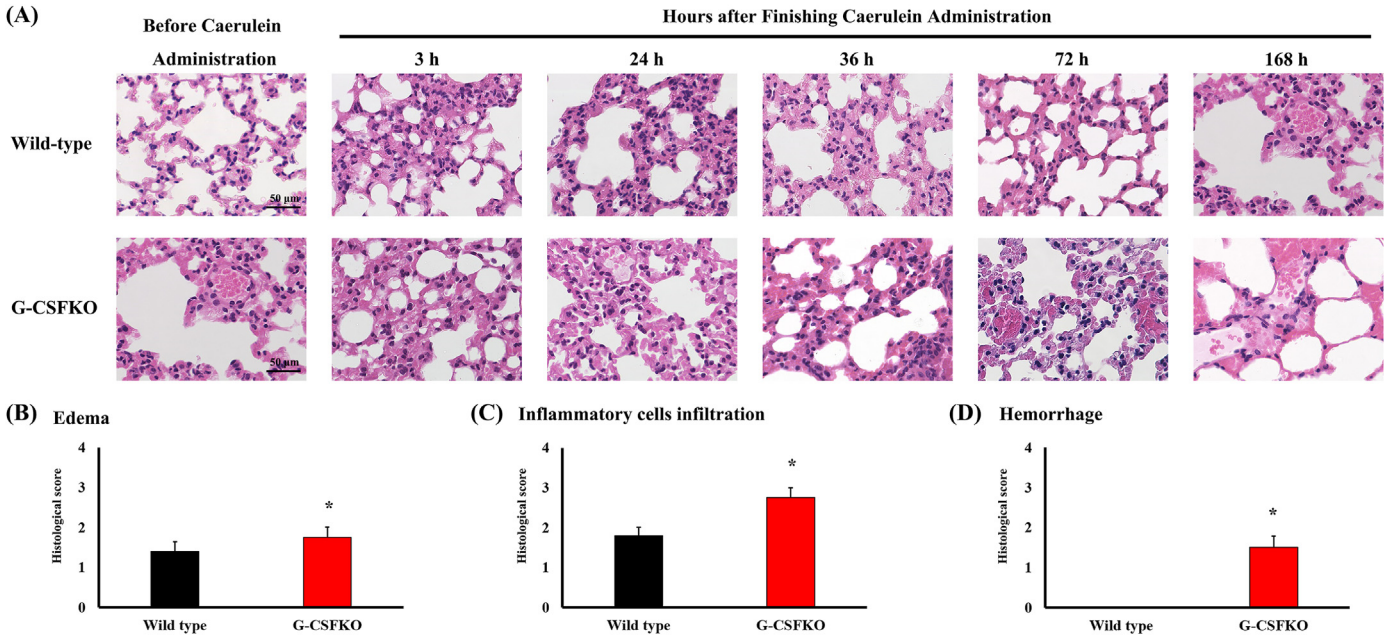

Fig. 5. Histological scores over time in lung in caerulein-induced pancreatitis mice.
A: Representative images of the lung over time after caerulein administration. Black arrows indicate edema. Yellow arrows indicate inflammatory cell infiltration.
B–D: Histological scores, pulmonary edema (B), inflammatory cell infiltration (C), and hemorrhage (D) over time in the lungs of caerulein-induced pancreatitis mice at 168 h after caerulein administration. *$P < 0.05$, versus the wild-type.

distant organs over time were determined (Fig. 5A). At 168 h after caerulein administration, inflammation in the pancreas was resolved in the wild-type mice, and edema, inflammatory cell infiltration, and bleeding were minimal in the lung (Fig. 5B–D). However, in the G–CSF–KO mice, the score was aggravated in the lungs 168 h after caerulein administration.

4. Discussion

Excessive neutrophil infiltration, as observed in severe systemic inflammatory reactions such as sepsis, is known to cause tissue destruction through excessive release of proteases into the extracellular matrix upon activation, in addition to their original bactericidal role. In particular, excessive degradation of extracellular matrices such as collagen, fibronectin, and laminin by overexpression of NE [22] has been implicated in the pathogenesis of various inflammatory diseases, including ARDS [3,9]. On the other hand, in a model of localized inflammation that eventually leads to spontaneous healing, such as that used in this study, innate immunity was shown to be mediated by neutrophils.

4.1. Neutrophil infiltration in the acute phase affects tissue dynamics in the chronic phase

In the pancreatitis model used in this study, serum amylase levels were measured over time in both G–CSF–KO and wild-type mice, and no differences were observed at any time point. This may indicate the absence of significant differences in the acute pancreatic cell damage caused by caerulein between G–CSF–KO and wild-type mice. In fact, the survival rate of G–CSF–KO mice increased from 96 h after caerulein administration, and the histological evaluation of edema, acinar necrosis, and inflammatory cell infiltration showed significant differences from 72 h after caerulein administration. In other words, various disorders in G–CSF–KO mice occurred late, after 72 h of caerulein administration. Three hours after the last caerulein administration, the number of neutrophils in G–CSF–KO mice was lower than that in wild-type mice, whereas the number of macrophages was higher, suggesting that G–CSF–KO mice have a compensatory mechanism.

4.2. Migration of cytotoxic lymphocytes: Differences between neutrophils and macrophages

CD8-positive T lymphocytes, which are cytotoxic T cells, are an important component of the adaptive immune system and play an important role in immune defense against intracellular pathogens such as viruses, bacteria, and tumors [23]. The fact that these cytotoxic T cells were significantly more abundant in the G–CSF–KO mice one week after the end of caerulein administration suggests that acute-phase tissue cleanup in the G–CSF–KO mice was insufficient despite the compensatory presence of macrophages in comparison with the wild-type mice. In other words, the results suggest that macrophages cannot compensate for the effects of neutrophils, since neutrophils perform a variety of effector functions, including phagocytosis, degranulation, release of reactive oxygen species (ROS), and neutrophil extracellular trap (NET) formation [2,24,25].

Likewise, the heterogeneity of neutrophils has also attracted attention in recent years, revealing characteristic phenotypes that may be dependent on neutrophil localization and health status [26]. One example is CxCR4+, VEGFR1+, and CD49d + angiogenesis-promoting neutrophils reported in mice and humans, which may be involved in extracellular matrix remodeling; however, the mechanisms underlying these differences remain unclear [27]. In G–CSF–KO mice, where neutrophils are virtually absent, these effects are thought to be lost. The effector functions of neutrophils are diverse, and perhaps a complex interplay of these effects, rather than a single action, results in the failure of tissue cleanup.

4.3. Expansion of inflammation to distant organs due to uncontrolled inflammation

Usually, when inflammation is limited or short-lived, the inflammatory response, such as vasodilation, chemical production, and leukocyte infiltration, in the inflamed tissue stops and damaged parenchymal cells regenerate. However, if injurious substances persist during acute inflammation, chronic inflammation occurs, and this process is characterized by long-lasting inflammation. Chronic inflammation is characterized by the presence of high numbers of macrophages and toxins, including ROS released by macrophages, resulting in the destruction of living tissues. In the G–CSF–KO mice in this study, the pancreas remained damaged due to the inability of neutrophils to function during the acute phase of inflammation. However, local inflammation did not converge and persisted, and the inflammation spilled over to multiple organs, which was thought to have contributed to the worsening of mortality. Neutrophils phagocytose not only pathogens but also injured cells and the extracellular matrix, and this phagocytosis is essential for the wound healing process. When the neutrophil count decreases, phagocytosis is reduced, and thus damaged cells and the extracellular matrix remain in the tissue without being removed. Thus, it is also assumed to delay wound healing because there is not enough space for fibroblasts, which promote fibrosis necessary for wound healing, to migrate. Such delayed healing is thought to spread to distant organs. In fact, G–CSF–KO mice in this study showed hemorrhage in lung tissue at 168 h after the end of caerulein administration, suggesting that the decrease in neutrophils may also contribute to the delayed convergence of inflammation that spills over to remote organs, which subsequently led to increased mortality in the G–CSF–KO mice in this study.

In systemic inflammatory diseases, such as sepsis, tissue destruction occurs due to excessive neutrophil migration and infiltration, and suppression of these factors can lead to tissue damage [8,9]. On the other hand, as shown in this study, neutrophils are extremely important for tissue repair. Regulation of the inflammatory response is critical for controlling inflammation, as it can be either too high or too low.

4.4. Study limitations

The increase in lymphocyte aggregation observed in G–CSF–KO mice during the chronic phase of inflammation was not examined in this study, because G–CSF–KO mice are deficient in G-CSF from birth. In addition, the direct effect of G-CSF on inflammation was not confirmed in the present study.

Funding

This study was supported in part by grants-in-aid for scientific research [numbers 22H03171, 22K09115, 22K16623, 22K16624, 21K09068, 21K16570, 20K17857, and 18K08914] from the Ministry of Education, Science and Culture of Japan.

Author contributions

Y.F. and K.M. wrote the manuscript; Y.F. and K.M. performed histopathological examinations; K.S., C.T., and H.F. performed immunohistochemical analyses; Y. Kawasaki, T. Minamiyama, A.S., N.T., and S.Y. assessed histological scores; A.N., T.S., R.K., A.U., A.K., Y. Kitagawa, T. F., T. Miyake, and T. Y. conducted the animal studies; N.T. and S.O. supervised the animal studies; H.O. and H.T. revised and edited the manuscript. All authors read and approved the final manuscript.

Declaration of competing interest

All authors declare no conflicts of interest.

Acknowledgments

We would like to thank Editage (www.editage.jp) for English language editing.

Appendix A. Supplementary data

Supplementary data to this article can be found online at https://doi.org/10.1016/j.pan.2023.10.020.

References

[1] Mestas J, Hughes CC. Of mice and not men: differences between mouse and human immunology. J Immunol 2004;172:2731–8. https://doi.org/10.4049/jimmunol.172.5.2731.
[2] Ley K, Hoffman HM, Kubes P, Cassatella MA, Zychlinsky A, Hedrick CC, et al. Neutrophils: new insights and open questions. Sci Immunol 2018;3. https://doi.org/10.1126/sciimmunol.aat4579.
[3] Abraham E. Neutrophils and acute lung injury. Crit Care Med 2003;31:S195–9. https://doi.org/10.1097/01.CCM.0000057843.47705.E8.
[4] Grommes J, Soehnlein O. Contribution of neutrophils to acute lung injury. Mol Med 2011;17:293–307. https://doi.org/10.2119/molmed.2010.00138.
[5] Donnelly SC, MacGregor I, Zamani A, Gordon MW, Robertson CE, Steedman DJ, et al. Plasma elastase levels and the development of the adult respiratory distress syndrome. Am J Respir Crit Care Med 1995;151:1428–33. https://doi.org/10.1164/ajrccm.151.5.7735596.
[6] Zemans RL, Colgan SP, Downey GP. Transepithelial migration of neutrophils: mechanisms and implications for acute lung injury. Am J Respir Cell Mol Biol 2009;40:519–35. https://doi.org/10.1165/rcmb.2008-0348TR.
[7] Li G, Jia J, Ji K, Gong X, Wang R, Zhang X, et al. The neutrophil elastase inhibitor, sivelestat, attenuates sepsis-related kidney injury in rats. Int J Mol Med 2016;38:767–75. https://doi.org/10.3892/ijmm.2016.2665.
[8] Fukuta T, Okada H, Takemura G, Suzuki K, Takada C, Tomita H, et al. Neutrophil elastase inhibition ameliorates endotoxin-induced myocardial injury accompanying degradation of cardiac capillary glycocalyx. Shock 2020;54:386–93. https://doi.org/10.1097/SHK.0000000000001482.
[9] Suzuki K, Okada H, Takemura G, Takada C, Kuroda A, Yano H, et al. Neutrophil elastase damages the pulmonary endothelial glycocalyx in lipopolysaccharide-induced experimental endotoxemia. Am J Pathol 2019;189:1526–35. https://doi.org/10.1016/j.ajpath.2019.05.002.
[10] Wang J. Neutrophils in tissue injury and repair. Cell Tissue Res 2018;371:531–9. https://doi.org/10.1007/s00441-017-2785-7.
[11] Schmidt J, Lewandrowski K, Fernandez-del Castillo C, Mandavilli U, Compton CC, Warshaw AL, et al. Histopathologic correlates of serum amylase activity in acute experimental pancreatitis. Dig Dis Sci 1992;37:1426–33. https://doi.org/10.1007/BF01296014.
[12] Gorelick FS, Thrower E. The acinar cell and early pancreatitis responses. Clin Gastroenterol Hepatol 2009;7(Supplement):S10–4. https://doi.org/10.1016/j.cgh.2009.07.036.
[13] Banks PA. Infected necrosis: morbidity and therapeutic consequences. Hepato-Gastroenterology 1991;38:116–9.
[14] Büchler MW, Gloor B, Müller CA, Friess H, Seiler CA, Uhl W. Acute necrotizing pancreatitis: treatment strategy according to the status of infection. Ann Surg 2000;232:619–26. https://doi.org/10.1097/00000658-200011000-00001.
[15] Fu CY, Yeh CN, Hsu JT, Jan YY, Hwang TL. Timing of mortality in severe acute pancreatitis: experience from 643 patients. World J Gastroenterol 2007;13:1966–9. https://doi.org/10.3748/wjg.v13.i13.1966.
[16] Ahmed Ali U, Issa Y, Hagenaars JC, Bakker OJ, van Goor H, Nieuwenhuijs VB, et al. Risk of recurrent pancreatitis and progression to chronic pancreatitis after a first episode of acute pancreatitis. Clin Gastroenterol Hepatol 2016;14:738–46. https://doi.org/10.1016/j.cgh.2015.12.040.
[17] Nøjgaard C, Becker U, Matzen P, Andersen JR, Holst C, Bendtsen F. Progression from acute to chronic pancreatitis: prognostic factors, mortality, and natural course. Pancreas 2011;40:119–200. https://doi.org/10.1097/MPA.0b013e318221f569.
[18] Lieschke GJ, Grail D, Hodgson G, Metcalf D, Stanley E, Cheers C, et al. Mice lacking granulocyte colony-stimulating factor have chronic neutropenia, granulocyte and macrophage progenitor cell deficiency, and impaired neutrophil mobilization. Blood 1994;84:1737–46. https://doi.org/10.1182/blood.V84.6.1737.bloodjournal8461737.
[19] Morishita K, Takemura G, Tsujimoto A, Kanamori H, Okada H, Chousa M, et al. Postinfarction cardiac remodeling proceeds normally in granulocyte colony-stimulating factor knockout mice. Am J Pathol 2015;185:1899–911. https://doi.org/10.1016/j.ajpath.2015.03.018.
[20] Langlois RA, Meyerholz DK, Coleman RA, Cook RT, Waldschmidt TJ, Legge KL. Oseltamivir treatment prevents the increased influenza virus disease severity

and lethality occurring in chronic ethanol consuming mice. Alcohol Clin Exp Res 2010;34:1425–31. https://doi.org/10.1111/j.1530-0277.2010.01226.x.
[21] Suzuki K, Okada H, Takemura G, Takada C, Tomita H, Yano H, et al. Recombinant thrombomodulin protects against LPS-induced acute respiratory distress syndrome via preservation of pulmonary endothelial glycocalyx. Br J Pharmacol 2020;177:4021–33. https://doi.org/10.1111/bph.15153.
[22] Owen CA, Campbell EJ. Neutrophil proteinases and matrix degradation. The cell biology of pericellular proteolysis. Semin Cell Biol 1995;6:367–76. https://doi.org/10.1016/s1043-4682(05)80007-8.
[23] Zhang N, Bevan MJ. CD8(+) T cells: foot soldiers of the immune system. Immunity 2011;35:161–8. https://doi.org/10.1016/j.immuni.2011.07.010.
[24] Rosales C. Neutrophils at the crossroads of innate and adaptive immunity. J Leukoc Biol 2020;108:377–96. https://doi.org/10.1002/JLB.4MIR0220-574RR.
[25] Yousefi S, Stojkov D, Germic N, Simon D, Wang X, Benarafa C, et al. Untangling "NETosis" from NETs. Eur J Immunol 2019;49:221–7. https://doi.org/10.1002/eji.201747053.
[26] Silvestre-Roig C, Fridlender ZG, Glogauer M, Scapini P. Neutrophil diversity in health and disease. Trends Immunol 2019;40:565–83. https://doi.org/10.1016/j.it.2019.04.012.
[27] Ng LG, Ostuni R, Hidalgo A. Heterogeneity of neutrophils. Nat Rev Immunol 2019;19:255–65. https://doi.org/10.1038/s41577-019-0141-8.